Rapid Rate of Tubulin Dissociation from Microtubules in the Mitotic Spindle In Vivo Measured by Blocking Polymerization with Colchicine

E. D. SALMON, M. McKEEL, and T. HAYS
Biology Department, University of North Carolina, Chapel Hill 27514

ABSTRACT At metaphase, the amount of tubulin assembled into spindle microtubules is relatively constant; the rate of tubulin association equals the rate of dissociation. To measure the intrinsic rate of dissociation, we microinjected high concentrations of colchicine, or its derivative colcemid, into sea urchin embryos at metaphase to bind the free tubulin, thereby rapidly blocking polymerization. The rate of microtubule disassembly was measured from a calibrated video signal by the change in birefringent retardation (BR). After an initial delay after injection of colchicine or colcemid at final intracellular concentrations of 0.1–3.0 mM, BR decreased rapidly and simultaneously throughout the central spindle and aster. Measured BR in the central half-spindle decreased exponentially to 10% of its initial value within a characteristic period of ~20 s; the rate constant, $k = 0.11 \pm 0.023\ s^{-1}$, and the corresponding half-time, $t_{1/2}$, of BR decay was ~6.5 ± 1.1 s in this concentration range. Below 0.1 mM colchicine or colcemid, the rate at which BR decreased was concentration dependent. Electron micrographs showed that the rapid decrease in BR corresponded to the disappearance of nonkinetochore microtubules; kinetochore fiber microtubules were differentially stable. As a control, lumicolchicine, which does not bind to tubulin with high affinity, was shown to have no effect on spindle BR at intracellular concentrations of 0.5 mM. If colchicine and colcemid block only polymerization, then the initial rate of tubulin dissociation from nonkinetochore spindle microtubules is in the range of 180–992 dimers per second. This range of rates is based on $k = 11\%$ of the initial polymer per second and an estimate from electron micrographs that the average length of a half-spindle microtubule is 1–5.5 μm. Much slower rates of tubulin association are predicted from the characteristics of end-dependent microtubule assembly measured previously in vitro when the association rate constant is corrected for the lower rate of tubulin diffusion in the embryo cytoplasm. Various possibilities for this discrepancy are discussed.

The metaphase mitotic spindle comprises two half-spindle arrays of microtubules that extend inwards towards the metaphase plate from opposite spindle poles, some microtubules overlapping in the metaphase plate region (1–7). Astral microtubules radiate outward from the centrosome complex at each spindle pole. Spindle and astral microtubules are in some form of steady-state equilibrium with a cellular pool of tubulin subunits, but the pathways of tubulin association–dissociation are unresolved (3, 8–14). Several measurements are available for the equilibrium and rate constants for the end-dependent polymerization–depolymerization of microtubules which occurs in in vitro reassembly buffers (15–26). However, the endogenous rates of tubulin association or dissociation with spindle microtubules have been unavailable for comparison.

For microtubules initially in equilibrium or at steady-state assembly, the dissociation rate constant can be measured by determining the rate of microtubule depolymerization that occurs when polymerization is abruptly blocked (18, 21, 23, 25). In principle, the tubulin-binding drug colchicine, or its derivative colcemid, can be used to block, abruptly and selectively, the polymerization of tubulin in living cells. Colchicine and colcemid bind tightly to a site on the tubulin dimer (27–

THE JOURNAL OF CELL BIOLOGY · VOLUME 99 SEPTEMBER 1984 1066-1075

33), which is not exposed when the dimer is assembled into microtubules in vitro (34–37). Colchicine penetrates sea urchin embryonic cells slowly; colcemid penetrates cells more rapidly, binds more rapidly than colchicine to the colchicine-binding site on brain tubulin (33) and, like colchicine, blocks microtubule elongation (28, 36). In either case, the intrinsic rate of tubulin dissociation for spindle microtubules will be revealed only when the drug concentration is sufficiently high that the rate of drug–dimer complex formation exceeds the rate at which unbound dimers associate into a microtubule. Above this drug concentration, the rate of microtubule depolymerization should be independent of concentration.

The inhibition of spindle microtubule assembly by exposure of cells to colchicine or colcemid before mitosis has been well documented. Several reports demonstrate that perfusion of cells with media containing colchicine or colcemid induces substantial disassembly of metaphase spindle microtubules within several minutes (38–40), but membrane permeability may be rate-limiting. In this regard, Hamaguchi (41) reported that mitotic spindles in sea urchin embryos lost most of their fibrous appearance in the extraordinarily short period of 30 s after the cells were microinjected with high concentrations (1 mM) of colchicine.

To measure the intrinsic rate of tubulin dissociation in spindle microtubules, we microinjected various concentrations of colchicine or colcemid into mitotic embryos of the sea urchin *Lytechinus variegatus*. Microinjection eliminated numerous problems that could be caused by membrane permeability. Measurements of the concentration of tubulin in the sea urchin embryo range from 5–27 μM (42–47). The amount of tubulin in the spindle and astral microtubules is normally 20% or less of the total tubulin (46). We used the quantitative injection technique of Hiramoto (48) and Kiehart (49) to produce 0.01–3.0 mM intracellular concentrations of colchicine or colcemid. Rapid changes in the assembly of spindle microtubules were analyzed from measurements of spindle birefringent retardation (BR)[1] obtained from video-voltage records by using a newly developed video analyzer system that recorded changes in BR as rapidly as 0.2 nm/s. BR has been shown to be proportional to the average amount of microtubule polymer along the measurement light path through the central half-spindle region between the chromosomes and the poles (50, 51). At high drug concentrations, nonkinetochore microtubule depolymerization followed a first-order decay, with a half-time of about 6.5 s. We calculated the initial tubulin dissociation rate to be 180–992 dimers/second per microtubule for the initial average length of a half-spindle microtubule estimated from electron micrographs to be 1.0–5.5 μm. This rate of dissociation is used to test the suitability of the in vitro end-dependent assembly characteristics to explain the kinetics of spindle microtubule assembly in the cellular environment.

MATERIALS AND METHODS

Biological Material and Polarization Microscopy: First, second, and third division embryos of the sea urchin *Lytechinus variegatus* were used. Methods for obtaining gametes, fertilization, culture, and the removal of fertilization membranes were as described by Salmon and Segall (52) and Salmon (53). Embryos were incubated in the injection chamber as described by Kiehart (49). The polarization microscope and procedures for visually measuring spindle BR using a Brace–Kohler compensator method were as described previously by Salmon and Ellis (54). A Nikon ×20 rectified objective (Nikon Inc., Garden City, NY) was used for video recordings and microphotography.

Microinjection Procedures: The microinjection process developed earlier by Hiramoto (48) and refined by Kiehart (49) was used to introduce colchicine rapidly into the cell. Fertilized sea urchin eggs were placed in a microinjection chamber as described by Kiehart (49). The eggs were sandwiched between a coverslip fragment and a coverslip to prevent their movement during the injection process. An aluminum support slide held the coverslip, coverslip fragment, and the surrounding seawater, which was capped with mineral oil to prevent evaporation.

The microinjection needles were made from glass capillary tubing (o.d. = 0.8 mm, i.d. = 0.6 mm, length = 100 mm, Drummond Scientific Co., Broomall, PA) using a micropipette puller (model MI, Industrial Science Assoc., Ridgewood, NY). The needles were loaded with mercury according to the methods developed by Hiramoto (48). A needle was attached to a pressure-driven syringe (2-ml model 81200, Roger Gilmont Instruments, Inc., Great Neck, NY) and set up on a micromanipulator (model M33, Brinkman Instruments, Inc., Westbury, NY) which was adjacent to the microscope. A capillary tubing reservoir that contained Wesson oil and the test solution was prepared as described by Kiehart (49) and placed on the support slide. An amount of Wesson oil (termed "measurement oil"), an equal amount of the test solution (10 or 100 mM colchicine, 10 mM colcemid, or 10 mM lumicolchicine), and a variable amount of capping oil were drawn sequentially into the needle from the reservoir. The loaded needle was then removed from the reservoir and maneuvered into the chamber containing the fertilized eggs. Generally, embryos that were at the one, two, or four-cell stage and had reached metaphase were selected for the injection.

At this stage, the video tape recorder was started, and the following procedures were monitored on the video screen. The needle was gently advanced into the egg with the tip projecting towards the mitotic spindle region, but not directly over the spindle. The outer Wesson oil cap and test solution were expelled rapidly into the cell. The needle was then quickly removed from the cell, and the remaining drop of measurement oil was expelled into the surrounding sea water.

The final concentration of test solution in each cell, C, was calculated using the cell volume, V_c, the volume of injected solution, V_i, and the concentration of the test solution, C_i, where $V_c = D_c^3\pi/6$, $V_i = D_i^3\pi/6$, and $C = D_i(D_i/D_c)^3$. D_i and D_c, the diameters of the drop of measurement oil and the unflattened cell, respectively, were measured from the recorded images on a video monitor. Distances were calibrated with a stage micrometer. The volume of injection solution was 0.5–4.4% of the cell volume.

Chemicals: Colchicine and colcemid were obtained from Sigma Chemical Co., St. Louis, MO. Most of the stock test solutions were made by dissolving colchicine or colcemid into distilled water. Occasionally, 10 mM PIPES, pH 6.9, was used instead as a solvent. Injection of the embryos 5% by volume with either distilled water or 10 mM PIPES, pH 6.9, had no effect on the spindle or on embryonic development. The maximum concentration of colchicine that we could dissolve in distilled water or 10 mM PIPES, pH 6.9, buffer was 100 mM; the maximum concentration of colcemid was 10 mM.

Several injections of 10 mM lumicolchicine (0.1–0.3 mM intracellular concentration) were performed as controls. Lumicolchicine was made by irradiating for 12 h a 10 mM colchicine stock with 366-nm light from a 100-W mercury arc lamp. The formation of lumicolchicine was confirmed by the disappearance of colchicine's absorption maximum at 350 nm (39).

Video Recording and Measurement of Changes in Spindle BR: Each microinjection experiment was recorded on video tape and played back later on a monitor (55–57). A Brace–Kohler compensator bias retardation of 11 nm was used. The image was recorded using a DAGE-MTI Newvicon camera, model 65S (DAGE-MTI, Inc., Michigan City, IN), a Vicon time date generator (Vicon Industries, Inc., Plainview, NY; model V240T), and a Sanyo VTR-1375 video time lapse tape recorder. Images viewed on a Sanyo VM4209 monitor were recorded photographically using Kodak Plus-X 35-mm film (Eastman Kodak Co., Rochester, NY). Changes in spindle BR were measured from the video records by measuring changes in the video voltage at corresponding regions of the spindle. For the data presented here, the video voltage at any selected position on the video raster was measured using a laboratory-built video analyzer in either the "spot meter" or "line scan" mode (Fig. 1). The video analyzer is similar in design concept to the Colorado Video model 321 video analyzer (Colorado Video, Inc., Boulder, CO).

We calibrated the video voltage to the magnitude of specimen BR using birefringent mica chips ~100 μm in size (Fig. 2). The mica chips were made by shearing pieces of mica in a Waring blender in a dilute aqueous suspension. The chips fracture along planes of several different thicknesses, hence they have different BR values. Images were recorded on video tape using the 11-nm compensator bias retardation employed in the recording of the biological

[1] *Abbreviation used in this paper:* BR, birefringent retardation.

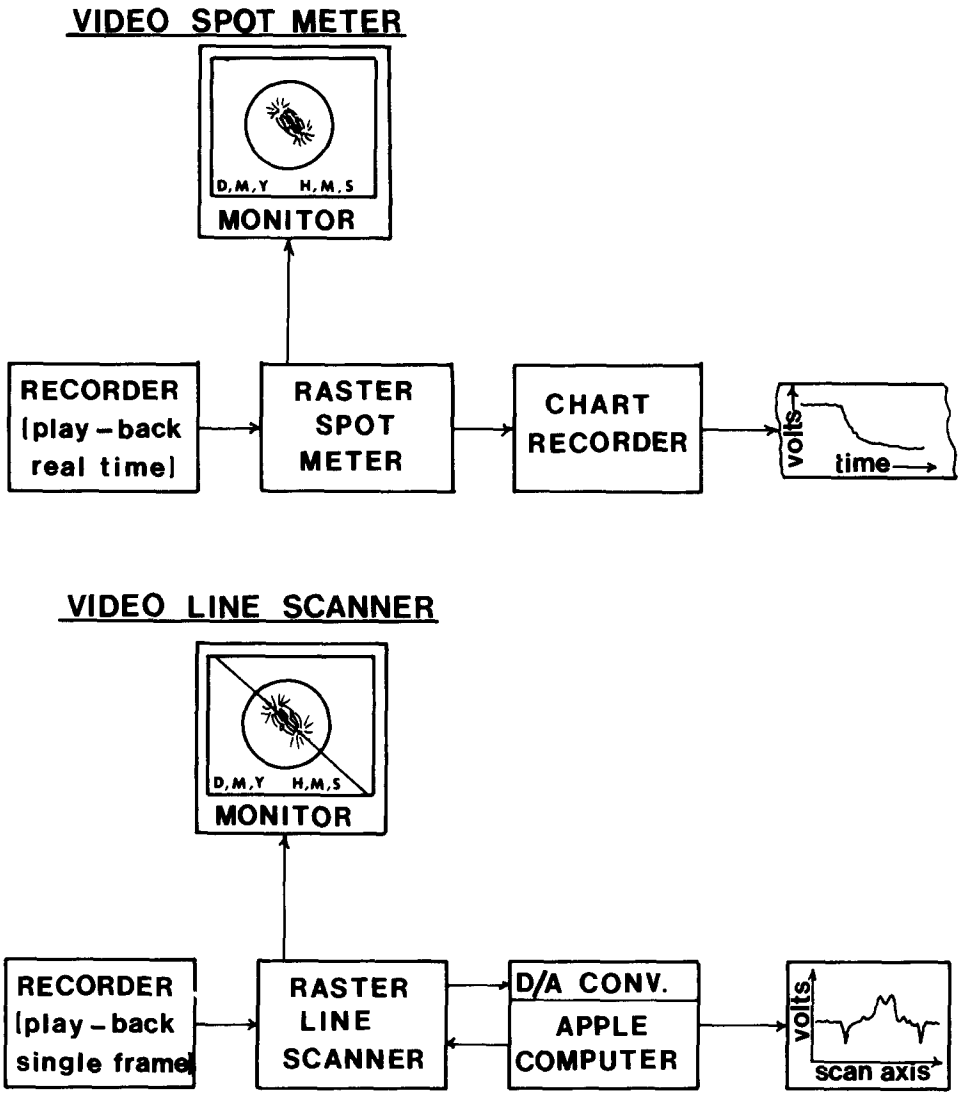

FIGURE 1 Measurement of spindle BR from the video voltage using (*a*) the video spot meter or (*b*) the video line scanner modes of the video analyzer. In the spot meter mode, the video voltage is sampled at a selected spot in the video field, corresponding to the position of a cursor on the image, and plotted on a strip chart recorder. In the line scan mode, the 256 video voltages along a straight cursor line are digitized as an 8-bit grey scale onto an Apple computer and plotted after scaling by an Epson printer. The position and orientation of the cursor line is selectable.

experiments. The difference in specimen voltage and background voltage due to the bias compensation ($V_S - V_B$) was measured and plotted against the value of BR determined by visual compensation methods as shown in Fig. 2. $V_S - V_B$ is proportional to specimen BR from 0 to 3 nm when the camera is operated with gamma correction using the manual pedestal and gain modes. The auto pedestal or black mode can also be used providing the blackest part of the video field remains constant during the experiments.

We measured the rate of spindle microtubule depolymerization after injection of colchicine or colcemid from video voltage recordings by using the "spot meter" mode of the video analyzer (Fig. 1). In the "spot meter" mode, a spot cursor, 1 video line-pair square, was placed on the image of the mitotic spindle in the central half-spindle region, about halfway between the spindle pole and the metaphase plate. The output voltage, $V_S(t)$, from the video analyzer's track-hold circuitry was recorded on a strip-chart recorder (model 355, Linear Systems Corp., Irvine, CA) at 6 cm/min while the video record was played back at original speed. The magnitude of V_B adjacent to the spindle region was also recorded. Spindle BR, measured by $V_S(t) - V_B$, was normalized by the BR at the time of injection.

In the video analyzer "line scan" mode (Fig. 1), the voltages along a cursor line aligned along the spindle's metaphase axis were digitized (model AI-02 8-bit digitizer, Interactive Structures, Bala Cynwyd, PA) into an Apple computer to analyze the changes in the profile of spindle fiber BR during microtubule depolymerization. Profiles for successive video images were plotted on an Epson MX-80 printer.

Electron Microscopy: We could not preserve spindle microtubules in untreated embryos by standard fixation methods, so we extracted embryos with an EGTA lysis buffer before fixing them for ultrastructural observations. Third division mitotic embryos were plunged rapidly into a 100-fold excess volume of seawater containing 10 mM colcemid. After 25 s the embryos were rapidly pelleted using a hand centrifuge, and at 45 s resuspended in an EGTA–glycerol lysis buffer containing 5 mM EGTA, 0.5 mM $MgCl_2$, 50 mM PIPES, pH 6.8, 20% glycerol (vol/vol), and 1% NP-40. This lysis buffer extracts the membranes and most ground cytoplasm from the embryos while stabilizing the assembled spindle microtubules, as described in detail by Salmon and Segall (52). After 10 min in the lysis buffer, samples were observed with polarization microscopy. Then the embryos were pelleted, resuspended in a 2% glutaraldehyde fixation buffer, and processed for thin-section electron microscopy (52). After lysis and fixation, the pattern of metaphase spindle BR was identical to the magnitude and distribution of BR in whole cells.

RESULTS

When living mitotic cells at metaphase or anaphase were injected with colchicine or colcemid at intracellular concentrations of 0.1–3.0 mM, BR was seen to decrease rapidly and simultaneously in both astral and central-spindle microtubules (Figs. 3*a* and 4). Usually, injection of the drug was complete in 1 s or less. After injection, there was a 1–5-s delay before the spindle BR began to drop. This delay represented, in part, the time required for diffusion of the drug through the cytoplasm and, in part, binding of the drug to tubulin. The closer the microneedle was to the spindle region, the shorter was the delay. After this initial delay, spindle BR decreased rapidly. In ~20 s, astral BR disappeared completely, while BR in the half-spindles decreased to low levels. The weak BR that remained in the half-spindles then disappeared very slowly over the next 10–15 min. Electron microscopy

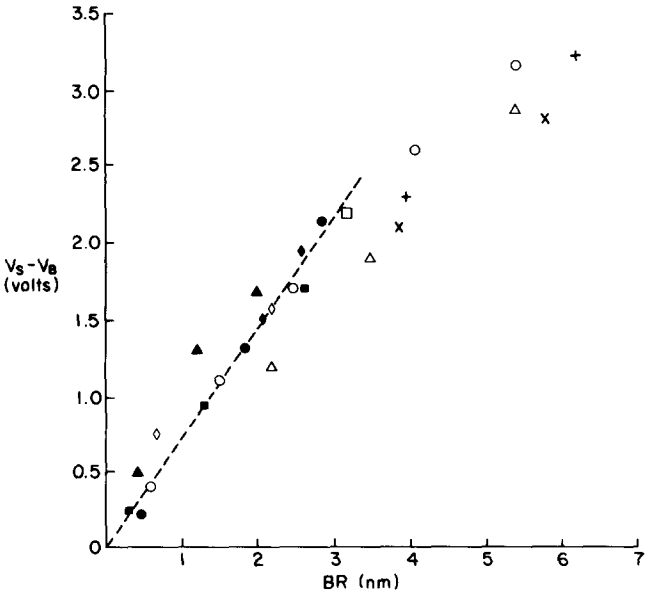

FIGURE 2 The relation between the video voltage and the magnitude of specimen BR. Mica chips of 100 μm or less in dimension were made by shearing large pieces of mica in distilled water using a Waring blender. These birefringent chips are split along fracture planes of different thickness. Chips with three or four clear planes of different BR (thickness) were used as specimens. For each chip the BR in nanometers was measured by visual compensation techniques for each plane; then the corresponding video voltage (V_S) was measured using the video spot meter with a bias retardation of 11 nm produced by the compensator. The difference $V_S - V_B$, where V_B is the background video voltage due to the 11-nm bias retardation, is plotted against the BR measured by compensator methods; a different symbol is used for different chips. For 3 nm and below, $V_S - V_B$ is proportional to BR. Details of the camera and recording devices are given in the text.

showed that this persistent half-spindle BR corresponded to differentially stable kinetochore fiber microtubules (Fig. 5).

The rapid changes in BR could not be quantified by standard manual compensator methods, but we were able to take measurements from video recordings because the video voltage signal is proportional to the magnitude of spindle BR over the normal BR range of 0–3 nm, as detailed in Materials and Methods. We quantitated the profile of BR changes along the spindle's interpolar axis (the cylindrical axis of symmetry) using the "line scan" mode of the video analyzer. (See Fig. 6 for BR profiles along the interpolar axes of the spindles in Figs. 3*a* and 4.) The spindle BR profiles measured by the video image processing techniques used here are comparable to the profiles measured by Hiramoto and co-workers using photomultiplier instrumentation (51). For both metaphase and anaphase spindles, the decay of spindle BR was mostly uniform throughout the half-spindle (Fig. 6). In anaphase spindles (Fig. 6*b*), as contrasted to metaphase spindles (Fig. 6*a*), there was a more distinct shift of the maximum rate of decay of BR from the equatorial region towards the poles as disassembly proceeded, but for either stage the great majority of BR decreased simultaneously throughout the half-spindle.

To quantitate the effect of drug concentration on the rate of microtubule depolymerization, we measured the change in BR in the center of the half-spindle using the "spot meter" mode of our video analyzer. A tracing of such a record is shown in Fig. 7*a* for the injection of colchicine to a final intracellular concentration of 0.2 mM. After the delay after injection, the BR decreased to 10% of its initial value within 25 s. The period after the initial delay, during which BR decreased to 10% of its initial magnitude, we defined as the characteristic time, τ, for the depolymerization of the nonkinetochore microtubules by a particular concentration of drug. In Fig. 8 the characteristic time, τ, is plotted as a function of intracellular drug concentrations from 0.01–5.0 mM. Below 0.01 mM, the spindle completed mitosis before the spindle disappeared. From 0.01–0.1 mM, the higher the drug concentration, the lower was the value of τ. From 0.1–5.0 mM, τ was ~20 s independent of the concentration of colchicine.

Values for τ approaching 20 s were also observed in perfusion experiments with colcemid. Perfusion of first-division mitotic cells with seawater that contained 10 mM colcemid resulted in a value of τ of ~45 s. By using later division mitotic cells (8–64 cell stages), where the surface to volume ratio is much greater, we achieved values of τ for perfusion with colcemid that approached the injection results (Fig. 8, △). Perfusions were also performed with podophylotoxin and nocodazole, two other drugs that bind to the tubulin dimer and block polymerization (33, 34, 41, 58). From visual observations, τ = 40 s after perfusion of second division mitotic embryos with 50 μM podophylotoxin, and τ = 20–30 s after perfusions of first division mitotic cells with 10 μg/ml nocodazole in seawater.

The disassembly curves followed a first-order decay over a significant part of the reaction after the delay after injection of 0.1–5.0 mM intracellular concentrations of colchicine. As shown in Fig. 7*a*, the $\overline{BR}$ (t) data could be fit to an exponential curve of the form:

$$\overline{BR}(t) = (\overline{BR}_{t=0} - \overline{BR}_{t=\infty})e^{-kt} + \overline{BR}_{t=\infty}, \qquad (1)$$

where $\overline{BR}(t)$ was spindle BR normalized by the initial magnitude at the time of injection, $\overline{BR}_{t=\infty}$ was the persistent weak $\overline{BR}$, $\overline{BR}_{t=0}$ equaled 1, time t was set equal to zero at the onset of BR decay, and the rate constant k was determined by exponential regression. The average value of $k = 0.11 \pm 0.023$ s^{-1} (14 samples) with an average coefficient of correlation of 0.992 ± 0.007. The corresponding half-time of BR decay, $t_{1/2}$ = 6.5 ± 1.1 s. The rate of depolymerization at high colchicine concentrations was rapid, but was only about 6 times faster than the rate at which half-spindle BR disappeared during normal anaphase (Fig. 7*b*).

As a control, we injected 0.5 mM intracellular concentrations of lumicolchicine into first-division mitotic embryos. Lumicolchicine has some of the same toxic side effects as colchicine, such as inhibition of nucleoside transport and binding to membranes, but it does not bind to tubulin (34). It had no effect on spindle structure or cell division (Fig. 3*b*).

DISCUSSION

The major finding reported here is the rapid depolymerization of nonkinetochore spindle and astral microtubules that occurs when tubulin polymerization is abruptly blocked by colchicine or colchicine-like drugs. After an initial delay, disassembly occurs simultaneously throughout the spindle and aster, and disassembly in the half-spindle follows a first-order decay with a half-time of ~6.5 s at higher drug concentrations. Kinetochore fiber microtubules, as expected from previous reports (59, 60 review), were differentially stable to the drug treatment. The discussion that follows concerns the assembly-

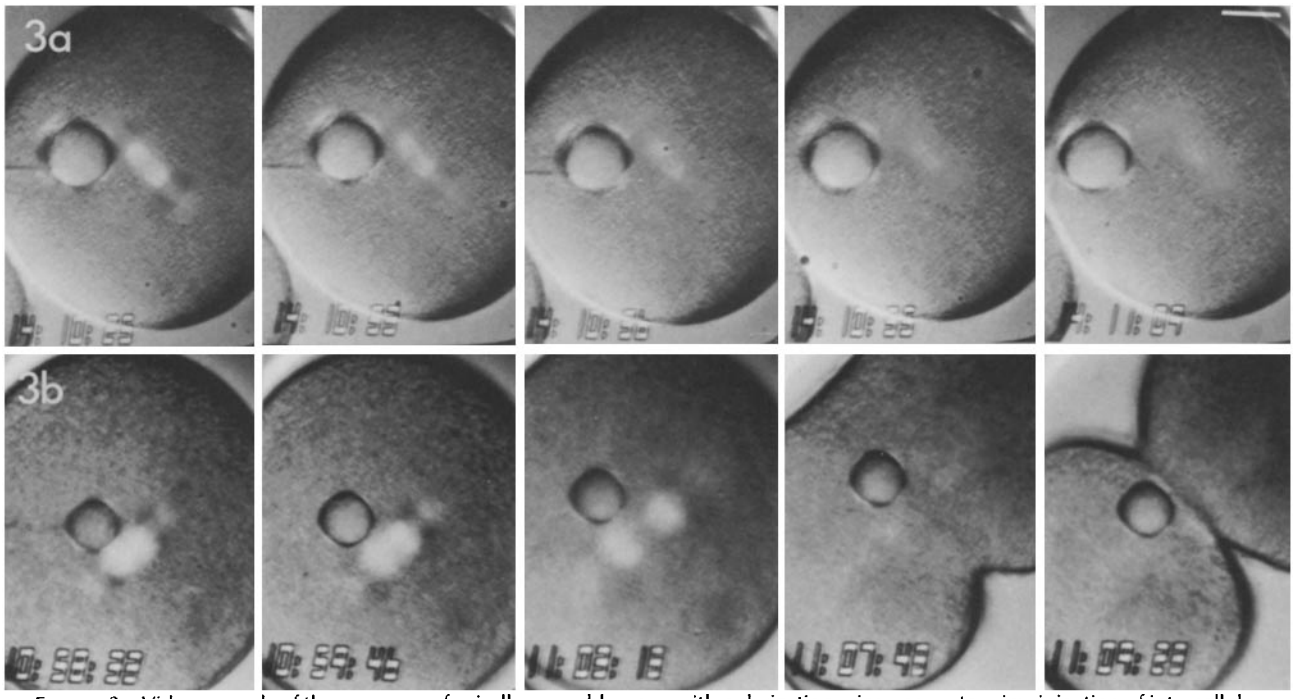

FIGURE 3 Video records of the response of spindle assembly, seen with polarization microscopy, to microinjection of intracellular concentrations of (*a*) 1.5 mM colchicine into a first-division metaphase embryo (*b*) and 0.75 mM lumicolchicine into a first-division metaphase embryo. Time in hours:minutes:seconds is given on each frame by the video time-date generator. In *a* note that most of the half-spindle and astral BR disappears in 20–25 s after injection. The BR remaining after 20–25 s corresponds to differentially stable kinetochore fiber microtubules (see text). Note that lumicolchicine has no effect on spindle assembly or cell division (*b*). Photographs were made from the video monitor. Bar, 30 μm. × 270.

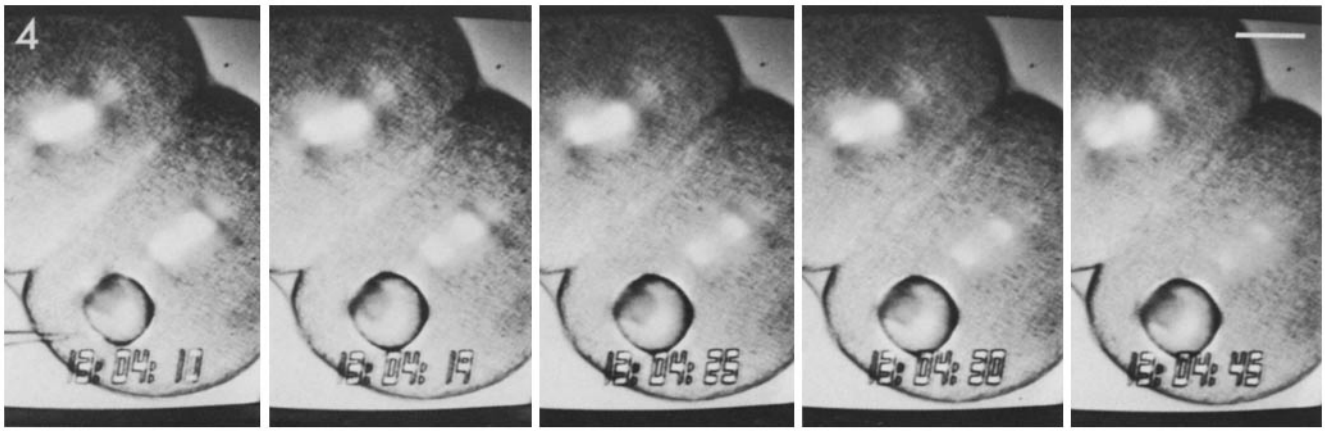

FIGURE 4 Microinjection of 0.75 mM intracellular concentration of colchicine into one cell of a second division, mid-anaphase embryo. Observations were recorded as described in the legend of Fig. 3. Like metaphase spindles, most of the half-spindle and astral BR disappears in 20–25 s after injection; only the differentially stable kinetochore fiber BR remains (see text). Note that the spindle in the noninjected cell is unaffected by colchicine injection into the neighboring cell. Bar, 30 μm. × 300.

disassembly pathways in the labile, nonkinetochore, spindle and astral microtubules.

The rapid rate of disassembly reported here is a measure of the native tubulin dissociation rate only if colchicine and colchicine-like drugs affect the assembly of spindle microtubules by forming a complex with the tubulin subunit that is incapable of polymerization. In vitro studies support this assumption. The colchicine-binding site on tubulin is not accessible in microtubules assembled in vitro from microtubule protein purified from brain, nor is it accessible in intact axonemal microtubules (34–37). Observations reported here also support this assumption. First, injection of equivalent concentrations of lumicolchicine had no effect on spindle BR and mitosis, as shown in Fig. 3*b*. Lumicolchicine does not bind tubulin dimers (28), thus should not have any effect on spindle assembly. Secondly, the variation in the rate of microtubule depolymerization as a function of drug concentration (Fig. 8) is consistent with the proposed binding mechanism; a limiting rate of depolymerization was observed at higher drug concentrations. At these concentrations, the rate of drug–tubulin complex formation appears to exceed significantly the rate of tubulin rebinding to microtubules.

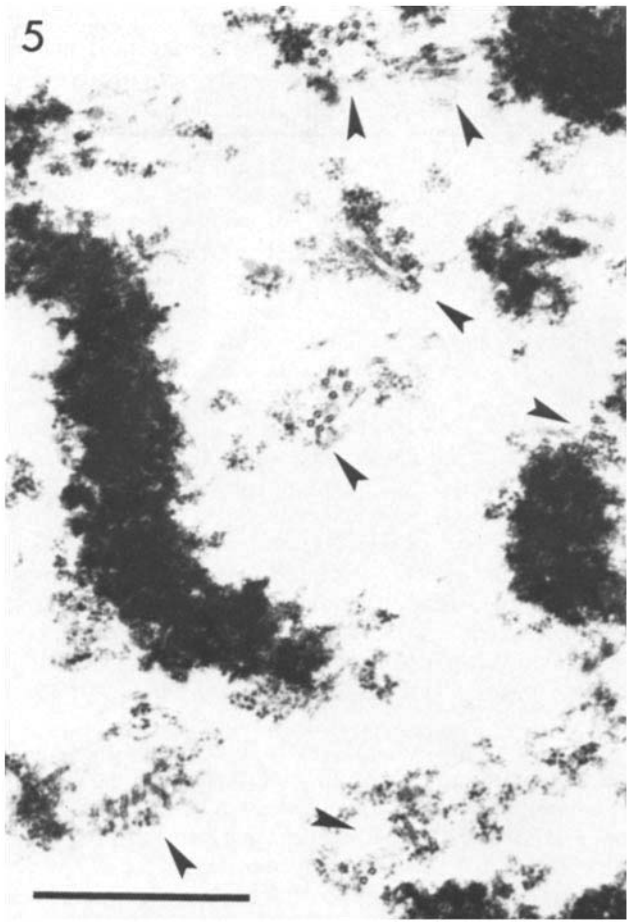

FIGURE 5 Electron micrograph of a cross section through the metaphase plate region of a third division metaphase spindle. Spindles were stabilized 45 s after 10 mM colcemid incubation using an EGTA-glycerol-NP-40 lysis buffer. In similar cross sections of untreated spindles, >200 microtubules are seen. In colcemid-treated spindles only bundles of kinetochore fiber microtubules are visible (arrows). In longitudinal sections, no astral nor nonkinetochore fiber half-spindle microtubules are seen. Bar, 1 μm. × 28,600.

Based on the uniformity of BR decay throughout the half-spindle (Figs. 3, 4, and 6), the first-order (or pseudo first-order) kinetics of $\overline{BR}$ decay measured in the central half-spindle region (Fig. 7*a*), and the proportional relation between BR and the amount of microtubule polymer along the measurement optical path through the spindle (50, 51), we conclude that the decrease in total microtubule polymer in the half-spindle after abrupt inhibition of assembly by high concentrations of colchicine follows first-order kinetics. In vitro, with reassembled brain microtubules, the decrease in total microtubule polymer, after abrupt inhibition of polymerization by dilution of the free tubulin pool, also follows first-order kinetics (23, 25, 61). This exponential decrease in the total polymer in vitro has been attributed to the constant rate at which tubulin subunits dissociate from microtubule ends and a length distribution of microtubules which is initially pseudo-exponential. A similar mechanism may explain the apparently exponential disassembly of the spindle that we measured in vivo, but the steady-state distribution of half-spindle microtubule lengths and the locations of microtubule ends within the half-spindle are not sufficiently well understood to test this hypothesis.

The in vivo tubulin dissociation rate constant, $k_{d(spindle)}$, per average length of nonkinetochore spindle microtubule, can be estimated from our measured rate constant, k = 11% of the initial polymer per second (25). The initial rate of tubulin dissociation is given by:

$$k_{d(spindle)} = 1{,}639\ kL_{av}, \qquad (2)$$

where L_{av} is the average initial microtubule length and 1,639 is the number of dimers per micrometer of microtubule. Unfortunately, the exact length distribution of half-spindle microtubules in situ for any higher eucaryotic cell is unknown. Nonkinetochore spindle microtubules are notoriously labile to fixation (52, 53), and the large number of microtubules in half-spindles (~3,000 for the sea urchin [50–52, 62, 63]) has prohibited detailed tracking studies. At this time we can only make a reasonable estimate of the value of L_{av}. In longitudinal sections aligned with the interpolar axis of isolated spindles, the microtubules in the half-spindle appear to extend from the spindle pole region towards the chromosomes, with the longer microtubules overlapping at the metaphase plate region (52, 53, 62, 63). A similar pattern of microtubule distribution is observed in mitotic spindles of cultured mammalian cells (1, 2, 4). We have reexamined 0.25-μm thick, longitudinal

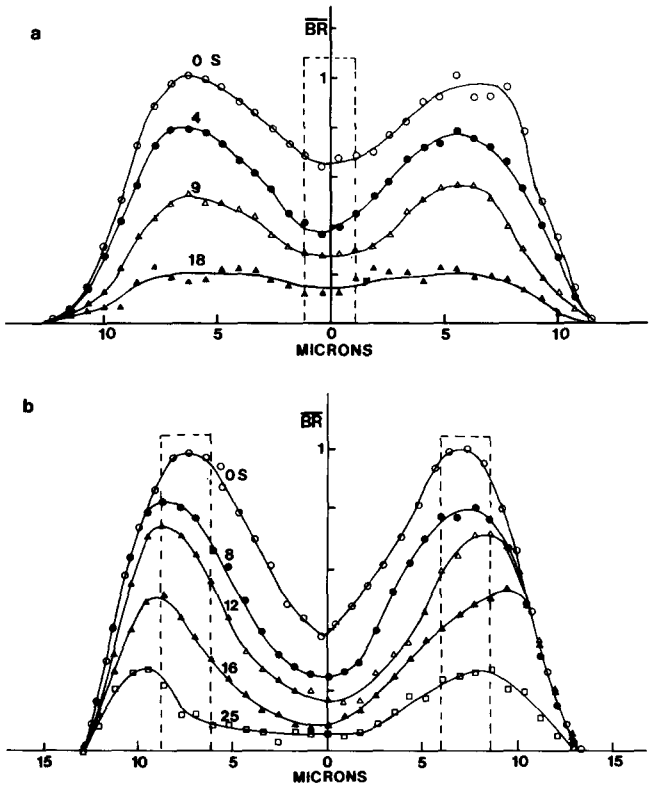

FIGURE 6 Changes in the profile of normalized spindle BR along the interpolar axis of (*a*) the metaphase spindle in Fig. 3*a*, and (*b*) the anaphase spindle shown in Fig. 4 after colchicine injection. Profiles were digitized using the line scan mode of the video analyzer from video images at times in seconds relative to the time of colchicine injection. Digitization was performed with the recorder in the "freeze frame" playback mode. At each time point, three successive video field tracings were averaged to reduce noise effects. Profiles at different times were aligned by eye and the family of spindle profiles plotted. The apparent positions of the chromosomes are indicated by the dotted line rectangles. Spindle BR, measured by $V_S - V_B$, is normalized by the peak central spindle BR at zero time for each spindle.

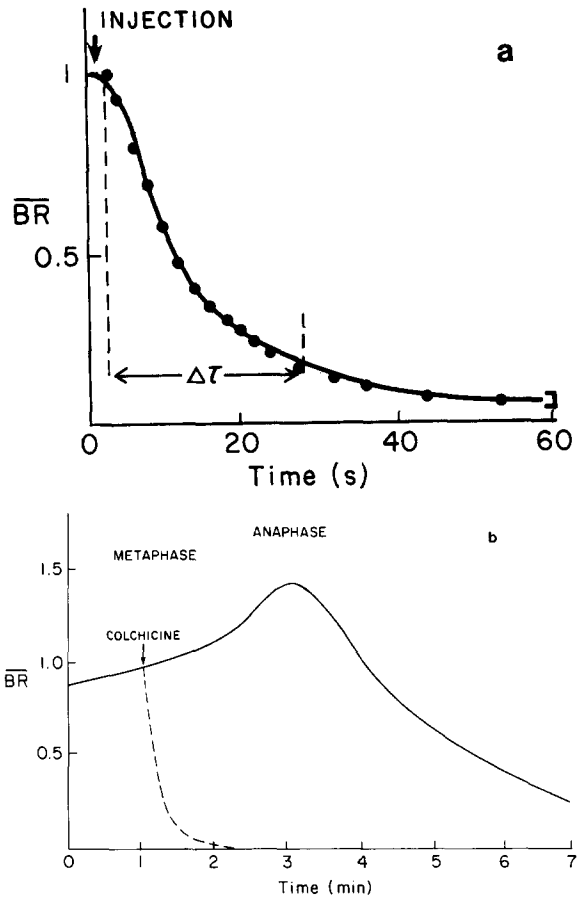

FIGURE 7 Changes in normalized spindle BR in the central half-spindle region as measured by the video spot meter from video recordings. (a) Tracing of the chart record of the changes in video voltage following injection of 0.2 mM intracellular colchicine into a first division metaphase cell. The characteristic time, τ, of nonkinetochore microtubule depolymerization is measured by the period between the time of onset of BR decay and the time where the video voltage decreases to 10% of the initial value before injection. The dotted line is a first-order decay curve derived from Eq. 1 for $k = 0.092$ and fitted to the data as described in the text. Spindle BR, measured by $V_S(t) - V_B$, is normalized by the initial value at the time of injection. The bracket shows the range of noise fluctuations in the original chart recordings. (*b*) Comparison of the rate of disapperance of normalized spindle BR after 1.5 mM intracellular colchicine injection with the normal rate of half-spindle disassembly at late anaphase.

sections of isolated metaphase spindles from sea urchin embryos obtained in a previous study (52). Most half-spindle microtubules appeared to be at least 1 μm long and the majority appeared to extend at least 5.5 μm, half the distance from the spindle pole region to the chromosomes. The thicker the section, the longer was the apparent length of the microtubules, but it is difficult to detect overlapping microtubule ends in dense microtubule bundles. Taking 1 μm as a minimum average length estimate and 5.5 μm as the more probable value, we calculate from Eq. 2 that $k_{d(spindle)}$ is in the range of 180–992 dimers per second.

This range of values of $k_{d(spindle)}$ is the same order of magnitude as the fastest rates of tubulin dissociation reported for microtubule disassembly in vitro in calcium-chelation buffers: 4.3–120 dimers per second for brain microtubule protein (17–21, 23–26, 61), 102–250 dimers per second for purified brain tubulin (22, 23, 61), and 10–55 dimers per second for purified axonemal tubulin from sea urchin sperm (26, 61). Unfortunately, no rate constants are available for sea urchin cytoplasmic or spindle tubulin. The origin of the dramatic variation in measured values for tubulin dissociation for brain microtubule protein is not clear, but may depend on the stabilizing action of high-molecular-weight microtubule-associated proteins (23, 26, 64) or the experimental methods used (26). In addition, very recent evidence indicates that the rate of tubulin dissociation in vitro, under nonsteady-state conditions where association is blocked, can be an order of magnitude or more faster than at steady-state equilibrium (61, 65).

Elevated Ca^{2+} ion concentrations, regulated by membrane components of the mitotic apparatus (49, 53, 63), may be responsible for the rapid tubulin dissociation rates observed in the present study. Karr and co-workers (24) have measured an end-dependent dissociation rate of tubulin from brain microtubules in vitro of 860 dimers per second in the presence of 5 mM Ca^{2+} ions. Microtubules depolymerize slowly over several minutes in mitotic spindles that have been isolated into calcium-chelation buffers, but they depolymerize within several seconds when the Ca^{2+} ion concentration is raised to 10 μM (52, 53).

Our estimate of $k_{d(spindle)}$ is derived from spindle disassembly measurements under nonsteady-state conditions and could be an overestimation of the steady-state tubulin exchange rate (61, 65). Is it reasonable to suppose that spindle microtubules can polymerize in vivo as rapidly as measured for depolymerization at high colchicine concentrations? Several studies show that the rate of assembly is at least 30% of our measured disassembly rate. Inoué and Sato (8) demonstrated that when 45% D_2O seawater was added to mitotic embryos of *L. variegatus* or other marine embryos, spindle BR doubled and spindle volume increased fivefold within 40 s. Microinjection of 100 mM taxol, which blocks tubulin dissociation (37, 55), into the mitotic spindle of *L. variegatus* can cause spindle BR to double over a 60-s period (DeSaix, P., and E. D. Salmon;

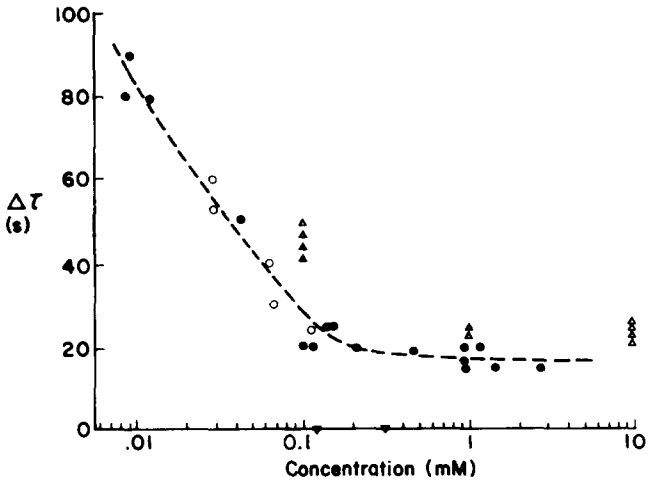

FIGURE 8 The variation of the characteristic time for nonkinetochore microtubule depolymerization, τ, with the intracellular concentration of injected colchicine (●) and colcemid (○). The data represented by the Δ symbols show the values of τ for 16–64 cell stage embryos for various colcemid concentrations in seawater perfusion buffers.

unpublished observations). Similar rapid rates of microtubule assembly are observed as spindles repolymerize after disassembly induced by application of cooling, hydrostatic pressure, or colcemid (8, 9, 11, 66). Microtubule assembly is a product of the kinetics of initiation as well as growth of microtubules. Thus the published rates of assembly in vivo are consistent within a factor of 2 or 3 with the rapid rate of microtubule depolymerization produced by high concentrations of intracellular colchicine. This rapid rate of tubulin association–dissociation is likely to be typical of the assembly of nonkinetochore mitotic spindle microtubules in higher eucaryotes. A characteristic time of 14 s for loss of spindle BR has been observed in mitotic spindles of PtK_1 culture cells when tubulin polymerization was blocked by 5–10 μg/ml nocodazole (Salmon, E. D., and M. Karow; unpublished observation), a drug that binds to tubulin at the colchicine-binding site (10, 58).

The next question we addressed is whether our estimated values of $k_{d(spindle)}$ are realistic for end-dependent association rates in the living cell. At steady-state equilibrium, the rate of dissociation is balanced by an equivalent rate of association which is the product of the concentration of tubulin in equilibrium with the microtubules, (T_c), the number of exchange sites per microtubule, and the bimolecular rate constants, k_a, for subunit addition to an exchange site. Values for k_a and (T_c) have been measured by several laboratories for the in vitro assembly of brain microtubule protein and purified tubulin (17–22, 26) and axonemal tubulin (26). Values for $k_{a(in\ vitro)}$, which are the sum of the k_a values measured for each end of the polymer, range from $1–20 \times 10^6\ M^{-1}\ s^{-1}$ at 30–37°C. Similarly, for the end-dependent assembly of actin filaments in vitro, values of $k_{a(actin)} = 7–10 \times 10^6\ M^{-1}\ s^{-1}$ have been reported (67). These values are similar to the fastest rates observed for several other protein–protein interactions and are thought to be close to the diffusion-limited reaction rate (68, 69).

The value of k_a in the embryo cytoplasm, $k_{a(embryo)}$, will be smaller than the in vitro measurements, in that the association rate constant is directly proportional to the diffusion coefficient (69). The diffusion coefficient of tubulin in sea urchin embryo cytoplasm has been measured recently using fluorescently labeled tubulin and fluorescence recovery after photobleaching techniques (70). The rate of diffusion is ~1/8–1/10 the rate that would be expected in the in vitro microtubule reassembly buffers (70a). Other globular proteins also have considerably lower diffusion rates in cytoplasm compared with dilute aqueous media (70–72). Taking the value of $k_{a(in\ vitro)}$ and correcting it for the lower diffusion rate of tubulin in the sea urchin cytoplasm, we estimate $k_{a(embryo)} = 0.1–2.5 \times 10^6\ M^{-1}\ s^{-1}$.

In vitro, the critical concentration (T_c) for brain microtubule protein is typically about 2 μM (13) at 30–37°C, for purified tubulin it is ~8 μM (22, 23), and for axonemal tubulin (T_c) is 1.8 μM (26). Although no values for the rate constant are available for the in vitro assembly of tubulin purified from sea urchin spindles, Keller and Rebhun (73) have recently measured (T_c) = 2 μM at 25°C for 6S tubulin purified from isolated sea urchin spindles. This value is less than half the estimated total tubulin concentration in the sea urchin embryo, measurements of which range from 5 to 27 μM (42–46, 74).

Assuming that the critical concentration of tubulin in the embryo is ~2 μM, we calculate $k_{a(embryo)}(T_c) = 0.2–5.0$ dimers per second. This result is substantially smaller than our experimentally observed $k_{d(spindle)} = 180–992$ dimers per second. Why doesn't the rate of spindle association predicted from parameters determined in vitro come close to matching the rate of spindle dissociation observed in our experiments with living cells?

One possibility to consider is that an oligomer of tubulin, not the dimer, is the basic tubulin subunit exchanging with the spindle microtubules. However, this suggestion is inadequate. For example, assume k_a is the same value for the oligomer as for the dimer. The rate of dissociation of the oligomer will be k_d/n where n is the number of dimers per oligomer, k_d is measured in dimers per second, and (T_c) is the dimer concentration in the cell. The value of (T_c) in the cell will be (T_c)/n but the rate of dissociation will be k_d/n. Thus there is no difference in the rates of association and dissociation. In fact, k_a for the oligomer is likely to be less than for dimer addition because the oligomer will have a lower diffusion coefficient.

Maybe the value of (T_c) determined for the in vitro assembly of microtubules does not adequately represent the situation in vivo. To balance a $k_{d(spindle)} = 180$ dimers per second, for $k_{a(embryo)} = 0.1–2.5\ M^{-1}\ s^{-1}$, ($T_c$) must be 72–1,800 μM. To balance a $k_{d(spindle)} = 992$ dimers per second, (T_c) must be 397–9,920 μM. Obviously, these values of (T_c) are much higher than the values determined for the in vitro assembly of microtubules. Even when we take the very highest estimated values of $k_{a(embryo)}$ ($2.5 \times 10^6\ M^{-1}\ s^{-1}$) and of cell tubulin concentration (27 μM), the product, 67 dimers per second, is significantly less than our experimental estimate of $k_{d(spindle)} = 180–992$ dimers per second. In addition, not all of the embryo's tubulin may be capable of assembly into the mitotic spindle (8, 9, 74, 75). The above analysis indicates that for an end-dependent assembly mechanism, the unpolymerized tubulin concentration in the spindle region may be substantially greater than predicted by the average cytoplasmic concentration.

If the concentration of assembly-competent, unpolymerized tubulin in the spindle region is not substantially greater than values of (T_c) measured in vitro, and $k_{d(spindle)}$ does represent the steady-state dissociation rate, then the above analysis indicates that spindle microtubule assembly is not strictly end dependent. This discrepancy lends support to Inoué's "dynamic equilibrium" theory which proposes that tubulin exchange occurs at sites along the entire length of spindle microtubules, not just at the ends (3, 8, 13, 14). Alternatively, microtubules at steady state in the living cell may be constantly breaking and reannealing, so that there are transiently many more functional ends than we would predict from studying electron micrographs of fixed spindles. The binding or release of protein or ions like Ca^{2+} (49, 52) could affect the stability of intertubulin binding in the microtubule wall; actin-binding proteins have been shown to serve a similar function in the fragmentation of actin filaments (76).

Nevertheless, the rapid depolymerization of spindle microtubules in vivo upon addition of 1 mM colchicine demonstrates that significant differences exist between the physiology of spindle microtubule assembly in the living cell and microtubule assembly in reassembly buffers in vitro. In the latter, colchicine-tubulin complexes bind to microtubule ends, blocking elongation, but do not induce rapid and extensive depolymerization (35, 36, 77, 78). A similar result is also found for the action of colchicine on the assembly of micro-

tubules in spindles isolated from sea urchin embryos into in vitro reassembly buffers (79). Colchicine at 1 mM concentrations has no effect on the rate of depolymerization of isolated spindle microtubules in the absence of exogenous tubulin; in the presence of exogenous tubulin, it blocks depolymerization (79). In vitro, the tubulin-colchicine complex has been demonstrated to bind only at microtubule ends (35, 77, 80), but the location of binding sites in vivo is undetermined (81).

The data and analysis presented here are not sufficient to define the pathways of tubulin exchange in living mitotic spindles. The analysis does show, however, that the characteristics of tubulin assembly-disassembly determined from experiments in vitro do not readily explain the observed behavior of mitotic spindles in vivo based on our current concepts of the distribution of microtubules in the spindle. Resolution of this dilemma will require more definitive data for the rate constants for spindle tubulin assembly in vitro, for the critical tubulin concentration in the spindle region, and the true length distribution of microtubules in the half-spindle. But it may also require some imaginative thinking about the fundamental processes in the living cell and how they may be altered by in vitro conditions.

We wish to thank Dick McIntosh, Shinya Inoué, Dick Weisenberg, Harold Erickson, Mike Caplow, George Langford, and Pat Wadsworth for their helpful discussion. Thanks to Nancy Salmon for her terrific editorial assistance.

This research was supported by grant GM-24364 from the National Institutes of Health.

Received for publication 6 July 1983, and in revised form 29 May 1984.

Note Added in Proof: Pat Wadsworth, working in our laboratory, has recently shown that the tubulin-colchicine complex is the active intermediate of the colchicine effects reported here. Microinjection of 40 μM tubulin-colchicine complex near the spindle region to give 2 μM or greater intracellular concentrations produced rapid loss of nonkinetochore spindle and astral BR with a characteristic time similar to the 20 s reported here for microinjection of high concentrations of colchicine.

REFERENCES

1. McIntosh, J. R., W. Z. Cande, and J. A. Snyder. 1975. Structure and physiology of the mammalian mitotic spindle. *In* Molecules and Cell Movement. S. Inoué and R. E. Stephens, editors. Raven Press, New York. 31.
2. Fuge, H. 1977. Ultrastructure of mitotic cells. *Int. Rev. Cytol.* 6 (*Suppl.*): 1–58.
3. Inoué, S. 1981. Cell division and the mitotic spindle. *J. Cell Biol.* 91 (No. 3, Pt. 2):131s–147s.
4. McIntosh, J. R. 1982. Mitosis and the cytoskeleton. *In* Developmental Order: Its Origin and Regulation. Alan R. Liss, Inc., New York. 77–115.
5. Euteneuer, U., and J. R. McIntosh. 1981. Structural polarity of kinetochore microtubules in PtK_1 cells. *J. Cell Biol.* 89:338–345.
6. Telzer, P. B., and L. T. Haimo. 1981. Decoration of spindle microtubules with dynein: evidence for uniform polarity. *J. Cell Biol.* 89:373–378.
7. Euteneuer, U., W. T. Jackson, and J. R. McIntosh. 1982. Polarity of spindle microtubules in *Haemanthus* endosperm. *J. Cell Biol.* 94:644–653.
8. Inoué, S., and H. Sato. 1967. Cell motility by labile association of molecules. *J. Gen. Physiol.* 50:259–292.
9. Salmon, E. D. 1975. Spindle microtubules: thermodynamics of in vivo assembly and role in chromosome movement. *Ann. N. Y. Acad. Sci.* 253:383–406.
10. De Brabander, M., G. Geuens, J. De Mey, and M. Joniau. 1981. Nucleated assembly of mitotic microtubules in living PtK_2 cells after release from nocodazole treatment. *Cell Motil.* 1:469–483.
11. Sluder, G. 1976. Experimental manipulation of the amount of tubulin available for assembly into the spindle of dividing sea urchin eggs. *J. Cell Biol.* 70:75–85.
12. Margolis, R. L., and L. Wilson. 1981. Microtubule treadmills—possible molecular machinery. *Nature* (*Lond.*). 293:705–711.
13. Inoué, S., and H. Ritter, Jr. 1975. Dynamics of mitotic spindle organization and function. *In* Molecules and Cell Movement. S. Inoué and R. E. Stephens, editors. Raven Press, New York. 3–30.
14. Fuseler, J. W. 1975. Temperature dependence of anaphase chromosome velocity and microtubule depolymerization. *J. Cell Biol.* 67:789–800.
15. Hill, T., and M. Kirschner. 1982. Bioenergetics and kinetics of microtubule and action filament assembly-disassembly. *Int. Rev. Cytol.* 78:1–125.
16. Scheele, R. B., and G. G. Borisy. 1981. In vitro assembly of microtubules. *In* Microtubules. K. Roberts and J. S. Hyams, editors. Academic Press, Inc., New York. 175–252.
17. Binder, L. I., W. L. Dentler, and J. L. Rosenbaum. 1975. Assembly of chick brain tubulin and flagellar microtubules from *Chlamydomonas* and sea urchin sperm. *Proc. Natl. Acad. Sci. USA.* 72:1122–1126.
18. Johnson, K. A., and G. G. Borisy. 1977. Kinetic analysis of microtubule self-assembly in vitro. *J. Mol. Biol.* 117:1–31.
19. Borisy, G. G. 1978. Polarity of microtubules in the mitotic spindle. *J. Mol. Biol.* 124:565–570.
20. Summers, K., and M. W. Kirschner. 1979. Characteristics of the polar assembly and disassembly of microtubules observed in vitro by darkfield light microscopy. *J. Cell Biol.* 83:205–217.
21. Bergen, L. G., and G. G. Borisy. 1980. Head-to-tail polymerization of microtubules in vitro. An electron microscope analysis of seeded assembly. *J. Cell Biol.* 84:141–150.
22. Cote, R. H., L. G. Bergen, and G. G. Borisy. 1980. Head-to-tail polymerization of microtubules in vitro: a review. *In* Microtubules and Microtubule Inhibitors. M. De Brabander and J. De Mey, editors. Elsevier/North-Holland Biomedical Press, Amsterdam. 325–338.
23. Karr, T. L., D. Kristofferson, and D. L. Purich. 1980. Mechanism of microtubule depolymerization. *J. Biol. Chem.* 255:8560–8566.
24. Karr, T. L., D. Kristofferson, and D. L. Purich. 1980. Calcium ion induces endwise depolymerization of bovine brain microtubules. *J. Biol. Chem.* 255:11853–11856.
25. Zeeberg, B., R. Ried, and M. Caplow. 1980. Incorporation of radioactive tubulin into microtubules at steady-state: experimental and theoretical analysis of diffusional and directional flux. *J. Biol. Chem.* 255:9891–9899.
26. Farrell, K. W., and M. A. Jordan. 1982. A kinetic analysis of assembly-disassembly at opposite microtubule ends. *J. Biol. Chem.* 257:3131–3138.
27. Wilson, L., and J. Bryan. 1974. Biochemical and pharmacological properties of microtubules. *Adv. Cell Mol. Biol.* 3:21–72.
28. Luduena, R. F. 1981. Biochemistry of tubulin. *In* Microtubules. K. Roberts and J. S. Hyams, editors. Academic Press, Inc., New York. 65–116.
29. Borisy, G. G., and E. W. Taylor. 1967. The mechanism of action of colchicine. Colchicine binding to sea urchin eggs and the mitotic apparatus. *J. Cell Biol.* 34:535–547.
30. Flaven, M., and C. Slaughter. 1974. Microtubule assembly and function in *Chlamydomonas*: inhibition of growth and flagellar regeneration by antitubulins and other drugs and isolation of resistant mutants. *J. Bacteriol.* 118:59–69.
31. Haber, J. E., J. G. Peloquin, H. O. Halvorsen, and G. G. Borisy. 1972. Colcemid inhibition of cell growth and the characterization of a colcemid-binding activity in *Saccharomyces cerevisiae*. *J. Cell Biol.* 55:355–367.
32. Engelborghs, Y., and A. Lambir. 1980. The physical chemistry of tubulin-colchicine interaction. *In* Microtubules and Microtubule Inhibitors. M. De Brabander and J. De Mey, editors. Elsevier/North Holland Biomedical Press, Amsterdam. 133–144.
33. Banerjee, A. C., and B. Bhattacharyya. 1979. Colcemid and colchicine binding to tubulin: similarity and dissimilarity. *FEBS* (*Fed. Eur. Biochem. Soc.*) *Lett.* 99:333–336.
34. Wilson, L., and I. Meza. 1973. The mechanism of action of colchicine. Colchicine binding properties of sea urchin tail outer doublet tubulin. *J. Cell Biol.* 58:709–719.
35. Margolis, R. L., and L. Wilson. 1977. Addition of colchicine-tubulin complex to microtubule ends: the mechanism of substoichiometric colchicine poisoning. *Proc. Natl. Acad. Sci. USA.* 74:3466–3470.
36. Deery, W. J., and R. C. Weisenberg. 1981. Kinetic and steady-state analysis of microtubules in the presence of colchicine. *Biochemistry.* 20:2316–2324.
37. Schiff, P. B., and S. B. Horwitz. 1981. Taxol assembles tubulin in the absence of exogenous guanosine 5-triphosphate or microtubule-associated proteins. *Biochemistry.* 20:3247–3253.
38. Inoué, S. 1952. The effect of colchicine on the microscopic and submicroscopic structure of the mitotic spindle. *Exp. Cell Res.* 2(*Suppl.*):305–318.
39. Aronson, J., and S. Inoué. 1970. Reversal by light of the action of *N*-methyl *N*-desacetyl colchicine of mitosis. *J. Cell Biol.* 45:470.
40. Sluder, G. 1979. Role of spindle microtubules in the control of cell cycle timing. *J. Cell Biol.* 80:674–691.
41. Hamaguchi, Y. 1975. Microinjection of colchicine into sea urchin eggs. *Dev. Growth Differ.* 17:111–117.
42. Raff, R. A., G. Greenhouse, K. W. Gross, and P. Gross. 1971. Synthesis and storage of microtubule proteins by sea urchin embryos. *J. Cell Biol.* 50:516–523.
43. Raff, R. A., and J. F. Kaumeyer. 1973. Soluble microtubule proteins of the sea urchin embryo: partial characterization of the proteins and behavior of the pool in early development. *Dev. Biol.* 32:309–320.
44. Burnside, B., C. Kozak, and F. C. Kafatos. 1973. Tubulin determination by an isotope dilution-vinblastine precipitation method: the tubulin content of *Spisula* eggs and embryos. *J. Cell Biol.* 59:755–762.
45. Pfeffer, T. A., C. F. Asnes, and L. Wilson. 1976. Properties of tubulin in unfertilized sea urchin eggs. *J. Cell Biol.* 69:599–607.
46. Sakai, H. 1978. The isolated mitotic apparatus and chromosome motion. *Int. Rev. Cytol.* 55:23–48.
47. Hiller, G., and K. Weber. 1978. Radioimmune assay for tubulin: a quantitative comparison of the tubulin content of different established tissue culture cells and tissues. *Cell.* 14:795–804.
48. Hiramoto, Y. 1974. A method of microinjection. *Exp. Cell Res.* 87:403–406.
49. Kiehart, D. 1981. Studies on the in vivo sensitivity of spindle microtubules to calcium ions and evidence for a vesicular calcium-sequestering system. *J. Cell Biol.* 88:604–617.
50. Sato, H., G. W. Ellis, and S. Inoué. 1975. Microtubule origin of mitotic spindle form birefringence: demonstration of the applicability of Weiner's equation. *J. Cell Biol.* 67:501–517.
51. Hiramoto, Y., Y. Hamaguchi, Y. Shoji, T. E. Schroeder, S. Shimoda, and S. Nakamura. 1981. Quantitative studies on the polarization optical properties of living cells. II. The role of microtubules in birefringence of the spindle of the sea urchin egg. *J. Cell Biol.* 89:121–130.
52. Salmon, E. D., and R. R. Segall. 1980. Calcium-labile mitotic spindles isolated from sea urchin eggs (*Lytechnius variegatus*). *J. Cell Biol.* 86:355–365.
53. Salmon, E. D. 1982. Mitotic spindles isolated from sea urchin eggs with EGTA lysis buffers. *Methods Cell Biol.* 25:69–105.
54. Salmon, E. D., and G. W. Ellis. 1976. Compensator transducer increases ease, accuracy, and rapidity of measuring changes in specimen birefringence with polarization microscopy. *J. Microsc.* 106:63–69.
55. Salmon, E. D., and S. Wolniak. 1983. Taxol stabilization of mitotic spindle microtubules: analysis using calcium-induced depolymerization. *Cell Motil.* 4:155–168.

56. Allen, R. D., J. L. Travis, N. S. Allen, and H. Yilmaz. 1981. Video-enhanced contrast polarization (AVEC-POL) microscopy: a new method applied to the detection of birefringence in the motile reticulopodial network of *Allogromia laticollaris*. *Cell Motil.* 1:275–294.
57. Inoué, S. 1981. Video image processing greatly enhances contrast quality and speed in polarization-based microscopy. *J. Cell Biol.* 89:346–356.
58. Hoebehe, J., G. Van Nijen, and M. De Brabander. 1976. Interaction of oncodazole (R17934), a new anti-tumoral drug, with rat brain tubulin. *Biochem. Biophys. Res. Commun.* 69:319–324.
59. Salmon, E. D., and D. A. Begg. 1980. Functional implications of cold-stable microtubules in kinetochore fibers of insect spermatocytes during anaphase. *J. Cell Biol.* 85:853–865.
60. Rieder, C. L. 1982. The formation, structure, and composition of the mammalian kinetochore and kinetochore fiber. *Int. Rev. Cytol.* 79:1–57.
61. Farrell, K. W., R. H. Himes, M. A. Jordon, and L. Wilson. 1983. On the nonlinear relationship between the initial rates of dilution induced microtubule disassembly and the initial free subunit concentration. *J. Biol. Chem.* 258:14148–14156.
62. Cohen, W. D., and L. I. Rebhun. 1970. An estimate of the amount of microtubule protein in the isolated mitotic apparatus. *J. Cell Sci.* 6:159–176.
63. Harris, P. 1975. The role of membranes in the organization of the mitotic apparatus. *Exp. Cell Res.* 94:409–425.
64. Murphy, D. B., K. A. Johnson, and G. G. Borisy. 1977. Role of tubulin-associated proteins in microtubule nucleation and elongation. *J. Mol. Biol.* 117:33–52.
65. Carlier, M., T. Hill, and Y. Chen. 1984. Interference of GTP hydrolysis in the mechanism of microtubule assembly: An experimental study. *Proc. Natl. Acad. Sci. USA.* 81:771–775.
66. Inoué, S., J. Fuseler, E. D. Salmon, and G. W. Ellis. 1975. Functional organization of mitotic microtubules. Physical chemistry of the in vivo equilibrium system. *Biophys. J.* 15:725–744.
67. Pollard, T. D., and M. Mooseker. 1981. Direct measurement of actin polymerization rate constants by electron microscopy of actin filaments nucleated by isolated microvillus cores. *J. Cell Biol.* 88:654–659.
68. Erickson, H., and D. Pantaloni. 1981. The role of subunit entropy in cooperative assembly: nucleation of microtubules and other two-dimensional polymers. *Biophys. J.* 34:293–309.
69. Koren, R., and G. G. Hammer. 1976. A kinetic study of protein-protein interactions. *Biochemistry.* 15:1165–1171.
70. Wojcieszyn, J. W., R. A. Schlegel, E.-S. Wu, and K. A. Jacobson. 1981. Diffusion of injected macromolecules within the cytoplasm of living cells. *Proc. Natl. Acad. Sci. USA.* 78:4407–4410.
70a. Salmon, E. D., W. M. Saxton, R. J. Leslie, M. L. Karon, J. R. McIntosh. 1984. Diffusion coefficient of fluorescein-labeled tubulin in the cytoplasm of embryonic cells of a sea urchin: measurement by video image processing of fluorescence redistribution after photobleaching. *J. Cell Biol.* In press.
71. Kreis, T. E., B. Geiger, and J. Schlessinger. 1982. Mobility of microinjected rhodamine actin within living chicken gizzard cells determined by fluorescence photobleaching recovery. *Cell.* 29:835–845.
72. Wang, Y.-L., F. Lanni, P. L. McNeil, B. R. Ware, and D. L. Taylor. 1982. Mobility of cytoplasmic and membrane-associated actin in living cells. *Proc. Natl. Acad. Sci. USA.* 79:4660–4664.
73. Keller, T. C. S., III, and L. I. Rebhun. 1982. *Strongylocentrotus purpuratus* spindle tubulin. I. Characterization of its polymerization and depolymerization in vitro. *J. Cell Biol.* 93:788–798.
74. Fulton, C., and P. A. Simpson. 1979. Tubulin pools, synthesis and utilization. *In* Microtubules. K. Roberts and J. Hyams, editors. Academic Press, Inc., New York. 117–174.
75. Stephens, R. E. 1972. A thermodynamic analysis of mitotic spindle equilibrium at active metaphase. *J. Cell Biol.* 57:133–147.
76. Bonder, E. M., and M. S. Mooseker. 1983. Direct electron microscopic visualization of barbed end capping and filament cutting by intestinal microvillar 95-kdalton protein(villin): a new actin assembly assay using *Limulus* acrosomal process. *J. Cell Biol.* 96:1097–1107.
77. Bergen, L. G., and G. G. Borisy. 1983. Tubulin-colchicine complex inhibits microtubule elongation at both plus and minus ends. *J. Biol. Chem.* 258:4190–4194.
78. Dietrich, H. W., and L. Wilson. 1983. Purification, characterization and assembly properties of tubulin from unfertilized sea urchin eggs of the sea urchin *Strongylocentrotus purpuratus*. *Biochemistry.* 22:2453–2462.
79. Hays, T., and E. D. Salmon. 1982. The action of colchicine on microtubules on isolated mitotic spindles. *J. Cell Biol.* 95:306*a*. (Abstr.)
80. Sternlicht, H., and I. Ringel. 1979. Colchicine inhibition of microtubule assembly via copolymer formation. *J. Biol. Chem.* 254:10540–10550.
81. Moll, E., B. Manz, S. Mocikat, and H.-P. Zimmerman. 1982. Fluorescent deacetylcolchicine. New aspects of its activity and localization in PtK-1 cells. *Exp. Cell Res.* 141:211–220.